

# A New Method of Potassium Chromate Production from Chromite and KOH-KNO<sub>3</sub>-H<sub>2</sub>O Binary Submolten Salt System

Zhi Sun, Yi Zhang, and Shi-Li Zheng

Key Laboratory of Green Process and Engineering, Institute of Process Engineering,  
Chinese Academy of Sciences, Beijing 100080, China

Yang Zhang

Key Laboratory of Green Process and Engineering, Institute of Process Engineering,  
Chinese Academy of Sciences, Beijing 100080, China

College of Chemistry and Chemical Engineering, Graduate University of Chinese Academy of Sciences,  
Beijing 100049, China

DOI 10.1002/aic.11871

Published online July 13, 2009 in Wiley InterScience (www.interscience.wiley.com).

*A new method of chromate production by applying a new reaction system of KOH-KNO<sub>3</sub>-H<sub>2</sub>O (binary submolten salt system) is proposed and proved feasible. Under conditions of temperature 350°C, KOH-to-chromite ore ratio 2:1, stirring speed 700 rpm, KNO<sub>3</sub>-to-chromite ore ratio 0.8:1, oxygen partial pressure 50%, and gas flow 1 L/min, chromium conversion ratio obtained is >98% with reaction time around 300 min. The decomposition of chromite ore in the system is a typical process of solid-liquid-gas reaction, which is coordinately controlled by mass diffusion in product layer and interface reaction. Apparent activation energy of decomposition in the temperature range from 280 to 370°C is 55.63 kJ/mol. During reaction, oxygen dissolves into KOH-KNO<sub>3</sub>-H<sub>2</sub>O melt system first and some cluster, e.g. O<sub>2</sub><sup>2-</sup>, is formed and the mass diffusion coefficient of the cluster was calculated. The system can be considered as both a media of oxygen transportation and reactant donator. Potassium nitrate plays a role of catalyst in the oxidation decomposition reaction of chromite ore and potassium hydroxide. © 2009 American Institute of Chemical Engineers AIChE J, 55: 2646–2656, 2009*

**Keywords:** chromite ore, potassium chromate, mechanism, decomposition, submolten salt

## Introduction

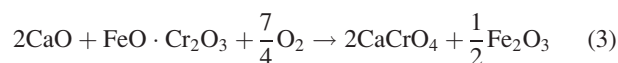
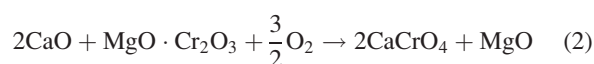
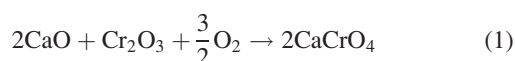
Pollutions from traditional chemical industries have been always threatening the environment severely.<sup>1</sup> They contaminate the water, destroy the soil, and dirty the atmosphere. To solve the problem, a great deal of effort has been devoted to process optimization and waste reduction.<sup>2</sup> However, pollution is usually inherent in the process itself. Therefore, from

the last several decades green chemistry has been proposed and applied in traditional chemical field.<sup>3,4</sup>

Chromate production is a highly important traditional industry providing basic and intermediate products for such industries as metallurgy, chemistry, and refractory, but its process is usually a major source of pollution.<sup>5</sup> Traditionally, chromite ore is processed with the addition of limestone and dolomite at about 1373 K in a kiln or rotary furnace, with low-utilization efficiency of resources and energy, producing a hazardous residue containing about 5% chromium, e.g. CaCrO<sub>4</sub>, which is harmful to the environment. Reactions 1–3 occur with the generation of CaO from limestone and

Correspondence concerning this article should be addressed to Y. Zhang at yizh@home.ipe.ac.cn

dolomite under the condition of traditional process. Once the  $\text{CaCrO}_4$  is airborne, it behaves as a further threat to all living beings because of its irritative, corrosive, and carcinogenic characters.<sup>6</sup>



To optimize the chromate making process, many attempts have been carried out based on the following purposes: higher utilization efficiency of chromite resource, lower reacting temperature, and lower chromium content in residue. Either hydrometallurgical or pyrometallurgical process is often used, especially acid or alkali leaching methods. Sulfuric acid is one of the common additives in the acid leaching of low-grade chromite to remove iron, aluminum, and other impurities to produce trivalent chromium compounds.<sup>7–9</sup> In alkali leaching, sodium carbonate is used as the main reactant.<sup>10</sup> The soda-ash roasting process has been commercially used for many years.<sup>11–13</sup> Frequently, sodium hydroxide is used because of its higher reactivity. In earlier reports, chromite ore was treated with molten sodium hydroxide under oxidizing conditions using air or oxygen, or even  $\text{NaNO}_3$ , to make sodium chromate.<sup>14–16</sup> In addition, oxychlorination and carbochlorination of chromite ore have been investigated.<sup>17–19</sup> However, all the aforementioned researches are only optimizations and never reducing pollutions from the viewpoint of green chemistry. Still, the environmental problem has not been resolved.

Recently, a novel KOH leaching process according to the principles of green chemistry, in which the recovery of chromium from chromite ore can be raised to above 99% and the residue amount reduced to 0.5 ton per ton product when compared with 2.5 ton in traditional processes, has recently been proposed by Zhang and coworkers.<sup>20–23</sup> A demonstration plant has been built in He'nan province, which has approached zero emission of chromium residue. The process has been named as submolten salt method ( $\text{KOH-H}_2\text{O}$ ) and attracted interesting from related research groups and industries worldwide and national financial supporting. In this article, we first proposed an additional new process named binary submolten salt method to produce  $\text{K}_2\text{CrO}_4$  from chromite ore by utilizing the lower molten point of  $\text{KOH-KNO}_3\text{-H}_2\text{O}$  to lower the amount of KOH in the leaching process and reduce the energy consumption. The effects of main factors, including KOH amount,  $\text{KNO}_3$  amount, oxygen partial pressure, flow amount, reaction temperature and time, and the reaction macrokinetics are investigated. In addition, the reaction mechanisms and  $\text{KNO}_3$  behavior are briefly discussed.

**Table 1. Chemical Analysis of –200-Mesh Vietnamese Chromite Ore**

Component	$\text{Cr}_2\text{O}_3$	FeO	MgO	$\text{SiO}_2$	$\text{Al}_2\text{O}_3$	$\text{MnO}_2$	CaO
Content, wt%	41.40	22.31	8.88	12.73	11.94	0.08	0.12

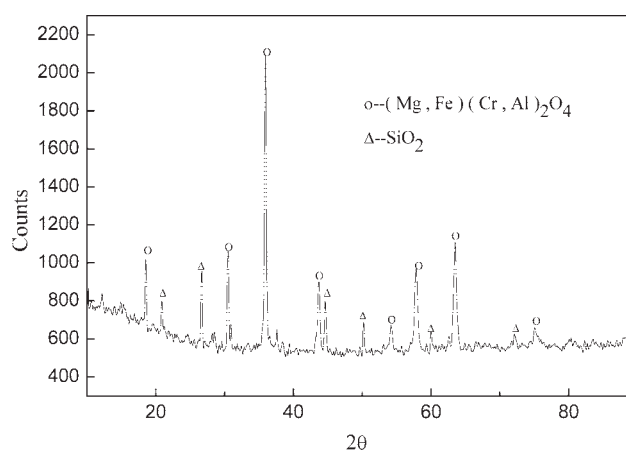


**Figure 1. XRD pattern of Vietnamese chromite ore.**

## Materials and Experiments

### Minerals

The chromite ore specimens originating from Vietnam were obtained from He'nan Zhenxing Chemical Group in China. The sample was dried overnight at  $110^\circ\text{C}$  and passed through –200-mesh sieves to obtain desired fractions for the extraction experiments. The chemical analysis of the Vietnamese chromite ore <200-mesh is given in Table 1 (composition varies but little with mesh size). The ratio of Cr to Fe in the chromite ore is 1.63 and the content of  $\text{SiO}_2$  is relatively high. Mineralogical analysis shown in Figure 1 indicates that Vietnamese chromite ore consists mainly of magnesiochromite and quartz.

The reagents potassium hydroxide and potassium nitrate employed in this work are of analytical grade and made by Beijing Chemical Plant. Distilled water was used throughout the experiments whenever needed.

### Experimental apparatus and procedure

All experiments were performed in a muffle furnace with a stainless steel open-top crucible (the volume is 1 L). Certain amount of KOH and  $\text{KNO}_3$  were first mixed in the crucible. Second, water was added making a mixture of  $\text{KOH-KNO}_3\text{-H}_2\text{O}$ . With the increase of temperature, the mixture formed a homogeneous liquid. When the temperature reached the setting value, the chromite ore prepared as already described was put in. During reaction, the system was fully mixed using a stirring machine (700 rpm). The viscosity of the melt is a very important factor that can impact the conversion ratio of chromium from chromite ore. However, the limitation of related data makes it hard to be quantified. The goal of the process is to optimize the energy consumption in our previous submolten salt process.<sup>21</sup> Therefore, little focus would be on the properties of the melt. After reaction, a separation procedure was performed to obtain liquid  $\text{KOH-KNO}_3\text{-H}_2\text{O}$  mother solution (with a salt mass ratio of about 50%), chromate crystal and ferric-rich residue. The temperature of the muffle furnace was controlled by a programmable temperature controller, with a precision of  $\pm 2^\circ\text{C}$ . The air to oxidize the chromite ore in the experiment was provided by an air compressor and

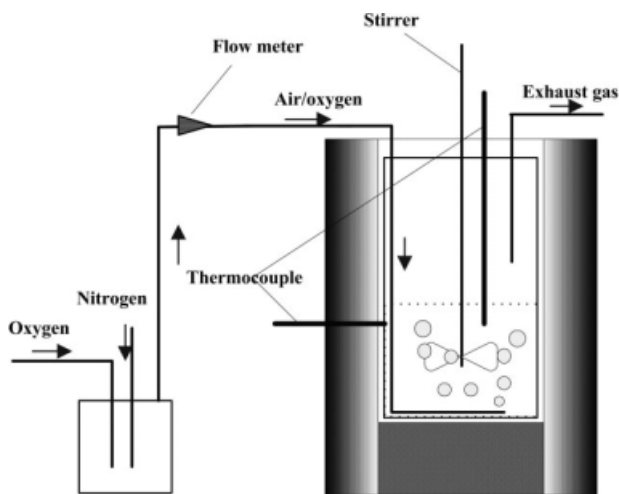


Figure 2. Graph of experimental apparatus.

controlled by a flow meter. In some cases, the oxygen or air flow was replaced by  $N_2$  to stop the reaction and the fusion products were cooled to room temperature for analysis. A schematic graph of experimental apparatus was shown in Figure 2. To gain the values of chromium conversion ratio from chromite ore to chromate, the residue was washed with hot distilled water carefully for at least four times and then dried at  $110^\circ\text{C}$  for 24 h. The mother solution, chromate crystal, and the solution for residue washing were also analyzed for Cr, Al, Si, and K. All experimental data were the average values of two or three parallel experiments. The fraction of chromium converted to potassium chromate was calculated using the expression:

$$\text{pct Conversion} = (1 - [\text{Cr}]_r/[\text{Cr}]_0) \times 100 \quad (4)$$

where  $[\text{Cr}]_r$  and  $[\text{Cr}]_0$  are the concentration of chromium in the residue and the concentration of chromium in the chromite ore, respectively.

$\text{NO}_3^-$ ,  $\text{NO}_2^-$  in the final products and contents of the exhaust gas were detected to examine the behavior of  $\text{KNO}_3$ .

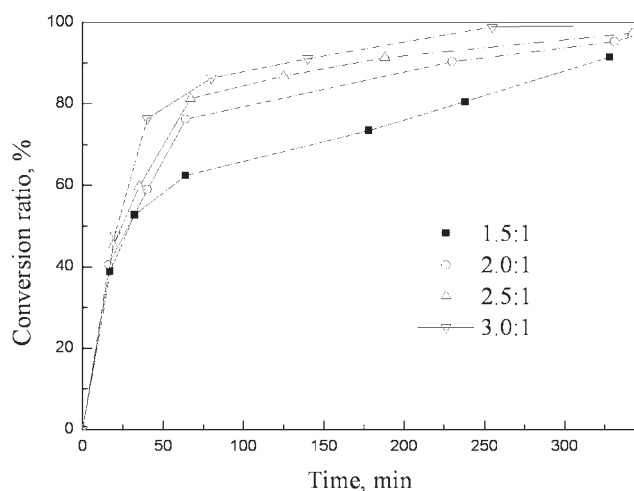


Figure 3. Effect of different KOH-to-ore ratios on chromium conversion ratio.

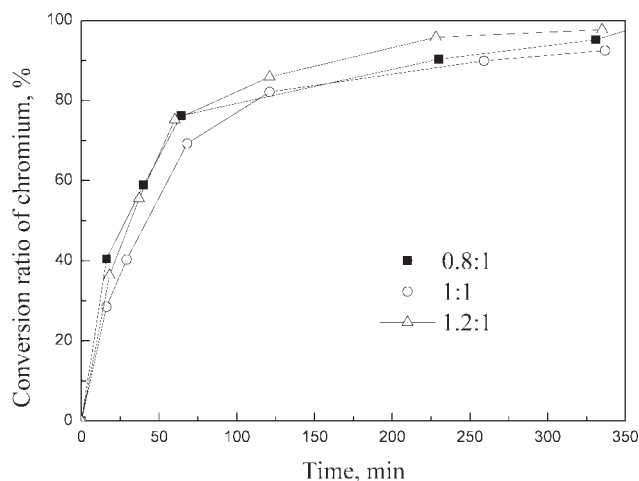


Figure 4. Effect of  $\text{KNO}_3$ -to-ore ratio on chromium conversion ratio.

### Chemical analysis and phase identification

The chromite ore, leaching solutions, and chromate crystal, residue were analyzed by ICP-OES (PE Optima 5300DV, PerkinElmer) and the phases with X-ray diffraction (XRD, Phillips PW223/30). Scanning electron microscopy (SEM) images of the chromite ore, crystal, and the residue were obtained with SEM (JEOL, Japan) equipment. The chromium content was also analyzed by volumetric titration to compare with the ICP-OES analysis. Water for analysis was super purified by a water super-purification machine (Milli-Q; Millipore).  $\text{NO}_3^-$  and  $\text{NO}_2^-$  in the final products were analyzed by ion-chromatogram (DX-500) and the exhaust gas by a gas analyzer (QUINTOX).

### Results and Discussion

This new method is based on the submolten salt method which has been described detailed in the related references.<sup>21</sup> By adding  $\text{KNO}_3$ , the amount of salt during processing chromite ore can be decreased and a binary submolten salt system generates. The Cr conversion ratios from chromite ore to chromate salt are obtained to determine the effects of different parameters in the new process.

#### Effect of KOH-to-chromite ore ratio

The amount of KOH using during reaction is an important factor, influencing mass transportation and its recycling amount in the whole process. In Figure 3, the effect of KOH-to-chromite ore ratio on chromium conversion ratio from chromite ore to potassium chromate is shown. Under the conditions of temperature  $350^\circ\text{C}$ , stirring speed 700 rpm,  $\text{KNO}_3$ -to-chromite ore ratio 0.8:1, oxygen partial pressure 50%, and gas flow 1 L/min, the conversion ratio jumps from 85% at 1.5:1 for 320 min to nearly 100% at 3:1 for 250 min. For different KOH-to-chromite ore ratios, very slight increase of conversion ratio at the first stage (from 0 to around 30 min) and apparently increase at latter stages of the reaction are observed. Combined with the effect of reaction time, it shows a typical result for a solid-liquid reaction, indicating the decrease of reaction surface area or the thickening of product layer of solid. At the first stage, no or very

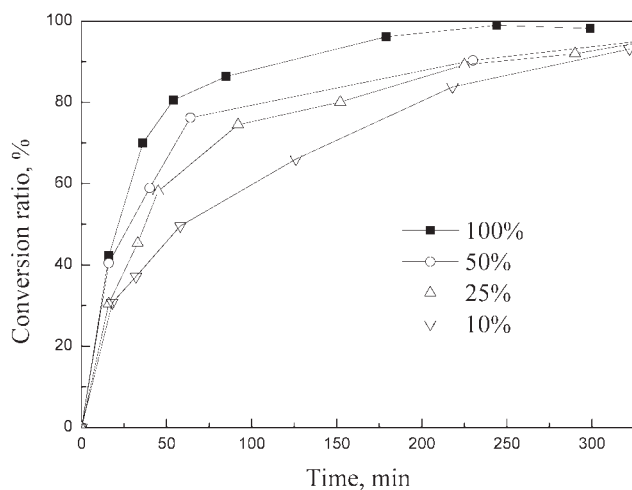
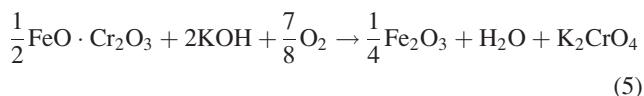


**Figure 5. Effect of oxygen partial pressure on chromium conversion ratio.**

thin product layer generates and therefore has little effect on the transportation of mass. With the increase of time, the solid product layer inhibits the diffusion of KOH and oxygen and a flat stage appears. On the other hand, the increase of KOH amount can enhance reaction as shown in Eq. 5.



#### Effect of KNO<sub>3</sub>-to-chromite ore ratio

According to the previous work, lowering KOH amount will increase reaction temperature due to inhibiting mass transportation.<sup>23</sup> Therefore, the addition of KNO<sub>3</sub> is aimed to form a lower melting point liquid (KOH-KNO<sub>3</sub>-H<sub>2</sub>O) and decrease the viscosity of the system. In Figure 4, the effect of KNO<sub>3</sub>-to-chromite ore ratio on chromium conversion ratio is investigated. The reaction conditions are of temperature 350°C, stirring speed 700 rpm, KOH-to-chromite ore ratio 2:1, oxygen partial pressure 50%, and gas flow 1 L/min.

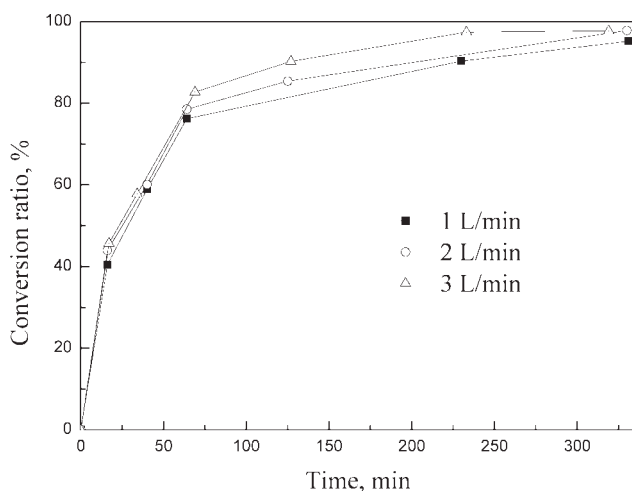


**Figure 6. Effect of flow meter on chromium conversion ratio.**

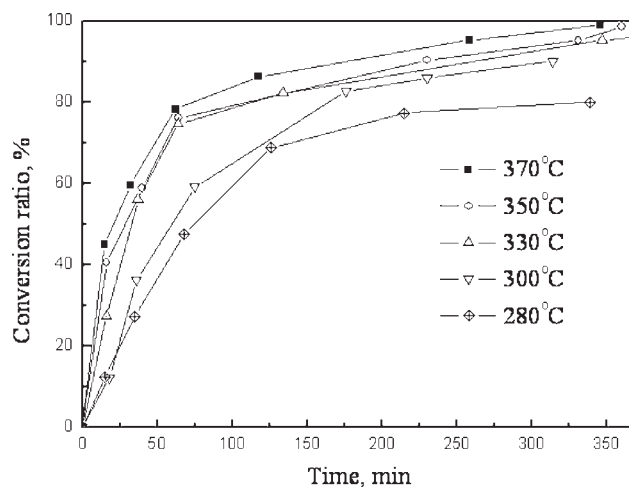


**Figure 7. Effect of temperature on chromium conversion ratio.**

There is obviously a counteracting behavior and an optimized value of KNO<sub>3</sub>-to-chromite ore ratio exists. During the decomposition of chromite ore, reactivity and viscosity of the system are two important factors that can determine the conversion ratio of chromium. In one case, the increase of potassium nitrate would decrease the reactivity of the system by diluting KOH concentration obtaining lower chromium conversion. In another case, the viscosity is decreased with the increase of KNO<sub>3</sub> amount which can enhance mass transportation during chromite ore decomposition. To reduce the recycling amount, KNO<sub>3</sub> should be added as few as possible. The one with lower potassium nitrate amount (0.8:1) shows faster reaction rate in the first stage of reaction, while lower rate in the later stage when mass diffusion dominates.

#### Effect of oxygen partial pressure

As shown in Eq. 5, oxygen is an important reactant playing the role of oxidizing Cr<sup>3+</sup> in chromite ore to soluble Cr<sup>6+</sup>. In the reaction conditions of temperature 350°C, stirring speed 700 rpm, KOH-to-chromite ore ratio 2:1, KNO<sub>3</sub>-to-chromite ore ratio 0.8:1, and gas flow 1 L/min, the effect of oxygen partial pressure (10, 25, 50, and 100%) on chromium conversion ratio is investigated and shown in Figure 5. The conversion can increase from 60% with oxygen partial pressure of 10% for 125 min to 86% with pure oxygen for 95 min. It indicates the increase of oxygen partial pressure can enhance oxygen transportation in the system of KOH-KNO<sub>3</sub>-H<sub>2</sub>O.

#### Effect of gas flow

Figure 6 shows the effect of gas flow (with different gas flow, 1 L/min, 2 L/min, and 3 L/min) on the conversion of chromium under the conditions of temperature 350°C, stirring speed 700 rpm, KOH-to-chromite ore ratio 2:1, KNO<sub>3</sub>-to-chromite ore ratio 0.8:1, and oxygen partial pressure 50%. In the first stage of reaction, no increase of conversion can be observed which indicates the mass diffusion playing less important role. However, as the thickening of solid product layer and decreasing of potassium hydroxide, mass



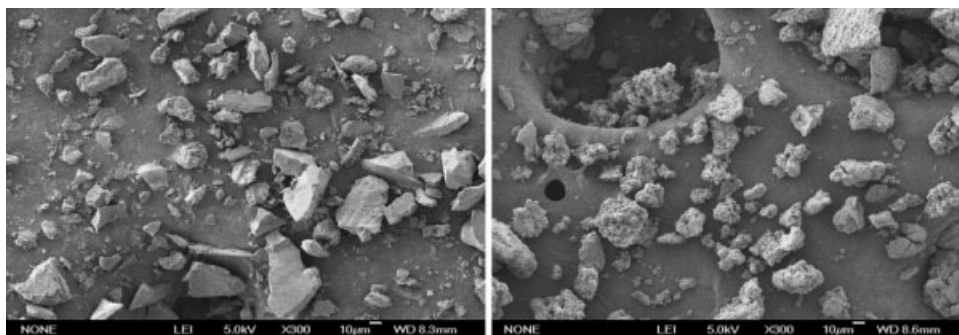


Figure 8. Comparison images of chromite ore and its resulting residue.

transportation or diffusion would become a dominate factor. Therefore, obvious increase of conversion is observed with the increase of gas flow in the later stage.

### Effect of temperature

Temperatures range from 280 to 370°C are investigated with other conditions of gas flow 1 L/min, stirring speed 700 rpm, KOH-to-chromite ore ratio 2:1, KNO<sub>3</sub>-to-chromite ore ratio 0.8:1, and oxygen partial pressure 50%. As related in Refs. 23 and 24, the increase of temperature can accelerate the decomposition of chromite spinel and change reactions equilibrium of the system. In Figure 7, chromium conversion shows clear temperature dependence. At 280°C, conversion is kept low, i.e. <80%, even with reaction time of 300 min. The increase of conversion can be observed in both first stage and later stage of reactions. However, the system (KOH-KNO<sub>3</sub>-H<sub>2</sub>O) becomes hard to control and water inside evaporates much faster.

### Macrokinetics of chromite ore decomposition

The temperature dependence of chromite ore decomposition can be used to estimate the apparent activation energy and elucidate the macrokinetics of the process, both helpful for reactor scale-up and project exercise. It is also a way to enclose the decomposition mechanisms. During the decomposition of chromite particle in KOH-KNO<sub>3</sub>-H<sub>2</sub>O after the

dissolving of oxygen, the following steps can be included: (1) the pseudo cluster from KOH and O<sub>2</sub> (the cluster is discussed in the later part) diffuses from the melt to the particle surface through the liquid boundary layer; (2) the cluster diffuses from the particle surface to the reaction interface through the residue layer; (3) Reaction 5 happens in the interface; (4) the chromate from Reaction 5 diffuses from the interface to the particle surface; and (5) the chromate diffuses from the particle surface to the melt. Because of the previous phase equilibrium results,<sup>25</sup> the solubility of potassium chromate decreases very fast due to the increase of salt concentration and a very small solubility reaches in the melt. Chromate can be considered in crystal state after reaction. The densities of the residue and crude crystal after separation are 1800 kg/m<sup>3</sup> and 2500 kg/m<sup>3</sup>, respectively, which mean they are very easy to be separated by gravity forces under the strong stirring conditions during the process. Therefore, only Steps 1–3 were considered.

During decomposition, chromite ore was attacked by KOH with progressive erosion of the spinel structure and resulted an amorphous-like residue (Figure 8). The corresponding XRD patterns and chemical composition are shown in Figure 9 and Table 2, respectively. Because of the comparison of chromite ore and its residue in Figure 8 and additional work about chromite ore processing, the decomposition of a chromite ore particle can be theoretically described by unreacted shrinking core model.<sup>24,26</sup>

The decomposition of chromite particle in the melt is a combination process of mass transfer, diffusion, and chemical reaction in macroscopic (Steps 1–3). To make the macro-mechanisms clearer, the mass transfer was considered separately. Because of the kinetics theory of gas–liquid–solid reaction,<sup>27</sup> Steps 1–3 can be derived by following.

Step 1, the pseudo cluster from KOH and O<sub>2</sub> diffuses from the melt to the particle surface through the liquid boundary layer. The mass flux  $r_L$  can be obtained by

$$r_L = 4\pi R_0^2 k_M (C_0 - C_s) \quad (6)$$

where  $k_M$  is the mass transfer coefficient of the cluster from KOH and O<sub>2</sub> in liquid boundary layer,  $R_0$  is the radius of the

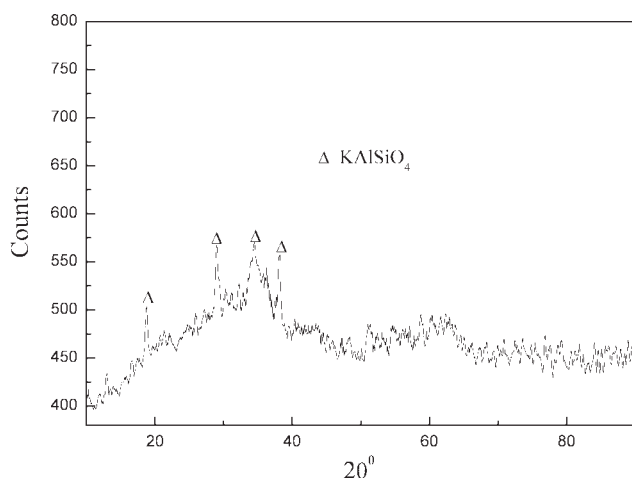
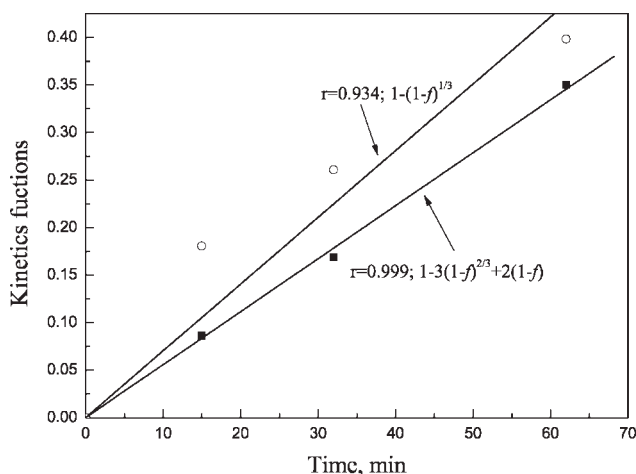


Figure 9. X-ray diffraction of chromium residue.

Table 2. Composition of the Chromium Residue

Contents	Cr	Fe	Mg	Mn	Al	Si	Ca	Ti	V	K
wt %	1.08	27.49	8.16	0.15	5.67	5.13	0.90	0.20	0.03	4.12



**Figure 10. Relationships between Cr leaching rate  $[1 - 3(1 - f)^{2/3} + 2(1 - f)]$  and time  $[1 - (1 - f)^{1/3}]$ .**

particle (the thickness of the liquid boundary layer can be neglected compared with the size of the particle in this case),  $C_0$  is the concentration of the cluster at  $t = 0$  and  $C_s$  is the concentration of the cluster on the surface of the particle.

Step 2, the cluster diffuses from the particle surface to the reaction interface through the residue layer. The mass flux  $r_p$  is

$$r_p = 4\pi r_i^2 D_e \left( \frac{dC}{dr_i} \right) = 4\pi D_e \frac{R_0 r_i}{R_0 - r_i} (C_s - C_i) \quad (7)$$

where  $r_i$  is the radius of the unreacted chromite core,  $D_e$  is the mass transfer coefficient of the cluster in the residue layer,  $C_i$  is the cluster concentration in the surface of the unreacted chromite core.

Step 3, Reaction 5 happens in the interface. The reaction is considered irreversible and estimated as pseudo first order reaction. The reaction rate  $v_i$  is

$$v_i = 4\pi r_i^2 k_{\text{rea}} C_i \quad (8)$$

where  $k_{\text{rea}}$  is the reaction rate constant.

In the case of stability, Eqs. 6–8 are equal and the main reaction rate  $r$  of chromite particle decomposition is obtained

$$r = \frac{4\pi R_0^2 C_0}{\frac{1}{k_M} + \frac{R_0(R_0 - r_i)}{D_e r_i} + \frac{1}{k_{\text{rea}}} \left( \frac{R_0}{r_i} \right)^2} \quad (9)$$

Because the radius of the unreacted chromite core  $r_i$  is hard to measure, the conversion ratio  $f$  obtained from Eq. 4 is used to replace the radius.

$$f = \frac{\frac{4}{3}\pi R_0^3 - \frac{4}{3}\pi r_i^3}{\frac{4}{3}\pi R_0^3} = 1 - \left( \frac{r_i}{R_0} \right)^3 \quad (10)$$

The amount of solid chromite core reacted via Reaction 5 in the time span of  $dt$  can be calculated from the main reaction rate.

$$r dt = -x \left( \frac{\rho}{M} \right) 4\pi r_i^2 dr_i \quad (11)$$

where  $\rho$  is the density of chromite particle,  $t$  is the reaction time,  $M$  is the molar weight of chromite ore, and  $x = 4$  can be obtained from Reaction 5.

Because of the aforementioned derivation, the relationship between the conversion ratio and the main reaction rate can be obtained as

$$\frac{df}{dt} = \frac{3M}{x\rho R_0} \frac{C_0}{\frac{1}{k_M} + \frac{R_0}{D_e} ((1-f)^{-1/3} - 1) + \frac{1}{k_{\text{rea}}} (1-f)^{-2/3}} \quad (12)$$

By integrating Eq. 12, the following equation is deduced

$$\begin{aligned} \frac{f}{3k_M} + \frac{R_0}{6D_e} [1 - 3(1-f)^{2/3} + 2(1-f)] \\ + \frac{1}{k_{\text{rea}}} [1 - (1-f)^{1/3}] = \frac{MC_0}{x\rho R_0} t \end{aligned} \quad (13)$$

where  $\rho = 4.5 \text{ g/cm}^3$  for chromite particle,  $R_0 = 3.7 \times 10^{-5} \text{ m}$  for 200 mesh,  $M = 223.8 \text{ g/mol}$ ,  $C_0 = 26.3 \text{ mol/L}$  when the weight ratio of KOH and  $\text{KNO}_3$  is 2:0.8.

At the first beginning when the conversion ratios are relatively small and the residue layer is very thin, the mass transfer in the liquid boundary layer is much more important than the mass diffusion in the residue layer. However, the reaction rate is normally very fast in the beginning during chromite ore decomposition and slows down after the residue layer forming, which makes the real mass transfer determined process is hard to be detected. To roughly evaluate the mass transfer of the cluster from KOH and oxygen, the method described in Ref. 28 was adopted by calculating the  $Sh$  number.

$$Sh = \frac{2k_M R_0}{D_{\text{KOH}}} = 2 + 0.95 Re^{1/2} Sc^{1/3} \quad (14)$$

where  $Re = \frac{2\rho_M v R_0}{\mu_M}$  and  $Sc = \frac{\mu_M}{\rho D_{\text{KOH}}}$ ,  $v$  is the mean velocity of the fluid around the chromite ore particle,  $\rho_M$  is the density of the melt,  $\mu_M$  is the viscosity of the melt, and  $D_{\text{KOH}}$  is the self diffusion coefficient of KOH in the melt.

Because of the absence of the properties of the melt  $\text{KOH-KNO}_3\text{-H}_2\text{O}$ , the data and methods from the related reference<sup>29</sup> were taken into account. The density  $\rho_M$  and viscosity  $\mu_M$  were estimated as  $1.75 \times 10^3 \text{ kg/m}^3$  and  $2.24 \times 10^{-3} \text{ Pa s}$  from the viscosities of KOH and  $\text{KNO}_3$  melt using a linear equation. The mean velocity of the melt around the chromite ore particle was estimated as  $0.3 \text{ m/s}$  for stirring velocity  $700 \text{ rpm}$  and impeller radius  $0.025 \text{ m}$ . The diffusion coefficient of KOH in the melt was estimated as  $1 \times 10^{-9} \text{ m}^2/\text{s}$ . Then, the mass transfer coefficient  $k_M$  through the liquid boundary layer around the chromite ore particle was calculated to be  $6.07 \times 10^{-4} \text{ m/s}$  according to Eq. 14.

With the increase of reaction time, the diffusion in the residue layer becomes dominated and the first part of Eq. 13 can be eliminated. To evaluate the process, the conversion data are substituted into different empirical macrokinetics equations from Eq. 13.<sup>27</sup> As shown in Figure 10, Eq. 16 has

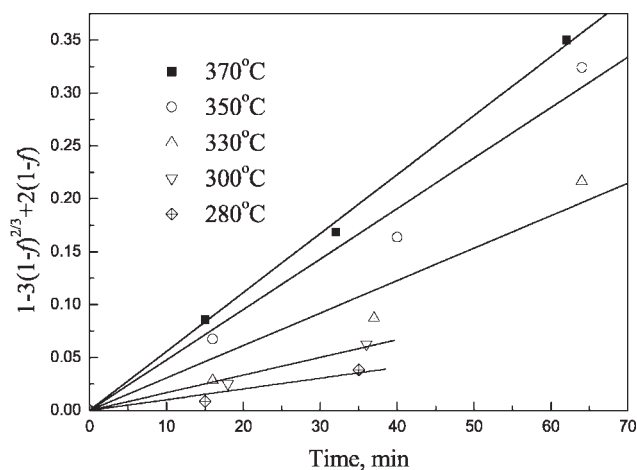


Figure 11. Plot of kinetics under various temperatures.

higher fitting relevance for the data at 370°C and the kinetics equation can be adopted to treat the experimental data.<sup>27</sup>

$$1 - (1 - f)^{1/3} = k_1 t \quad (15)$$

$$1 - 3(1 - f)^{2/3} + 2(1 - f) = k_2 t \quad (16)$$

where  $k_1$ ,  $k_2$  are the slopes of the fitted lines.

Conversion ratios for the first stage of the decomposition with different temperatures are fitted and calculated with Eq. 16 (Figure 11). The data are shown in Table 3. To calculate the mass diffusion coefficient, Eqs. 13, 16 were compared to obtain the following equation:

$$D_e = \frac{4\rho R_0^2}{6MC_0} k_2 \quad (17)$$

Figure 12 shows the temperature dependence of mass diffusion coefficient of the cluster from KOH and oxygen. The magnitude of rather small compared with the mass transfer coefficient through the liquid boundary layer. Therefore, mass diffusion in the residue layer is the determined step of the reaction. During the reaction, the mass diffusion of the cluster influences the decomposition of chromite particle and any method can improve inner mass diffusion in the residue layer can enhance the reaction, e.g., increase of temperature and decrease of particle size.

Then, the specific apparent activation energy of the main reactions, the specific apparent and an Arrhenius plot of the natural logarithm of reaction rate ( $\ln k_2$ ) against the reciprocal of

Table 3. Reaction Rate Constant and Mass Diffusion Coefficient at Different Temperatures

$T/^\circ\text{C}$	$T/\text{K}$	$1000/T/\text{K}^{-1}$	$k_2$	$\ln k_2$	$D_e, 10^{-14} \text{ m}^2/\text{s}$
370	643	1.554847	0.00561	-5.1832	6.5241
350	623	1.60475	0.00498	-5.30233	5.7914
330	603	1.657962	0.00341	-5.68104	3.9656
300	573	1.744744	0.00174	-6.35387	2.0235
280	553	1.807828	0.00112	-6.79443	1.3025

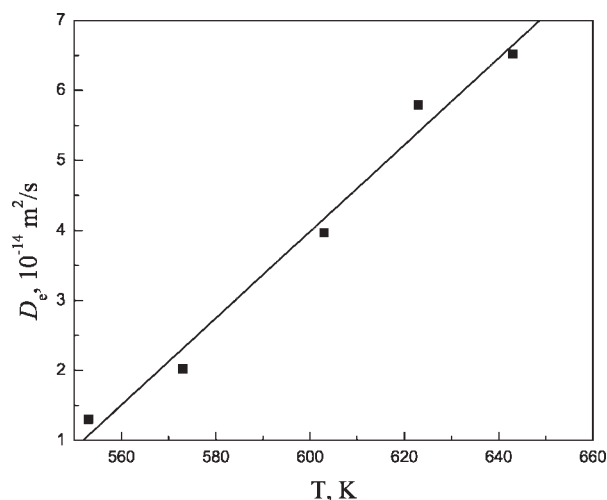


Figure 12. Temperature dependence of mass diffusion coefficient of the cluster from KOH and oxygen.

absolute temperature ( $1/T$ ) is made (Figure 13) based on Arrhenius equation (Eq. 18).

$$\ln k_2 = \ln A - \frac{E}{R} \times \frac{1}{T} \quad (18)$$

Because of Eq. 18 and the slope of the fitted line in Figure 11, the specific apparent activation energy  $E = 6691 \times R = 55.63 \text{ kJ/mol}$ . When compared with the Figure 12, it suggests the decomposition can be coordinately controlled by mass diffusion in the product (residue) layer and interface reaction.

To lower the recycling amount of potassium and ensure high-chromite ore utilization efficiency, the system should be carefully retained, i.e., the water content to ensure lower viscosity. For scaling up, following macrokinetics equation can be applied (Eq. 19).

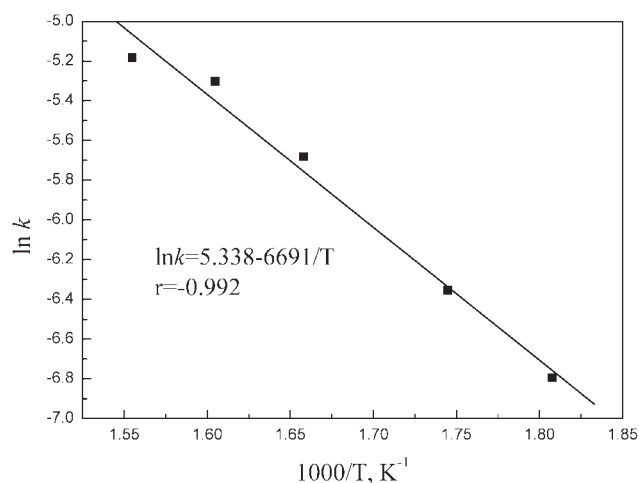


Figure 13. Natural logarithm of reaction rate constant versus reciprocal temperature.

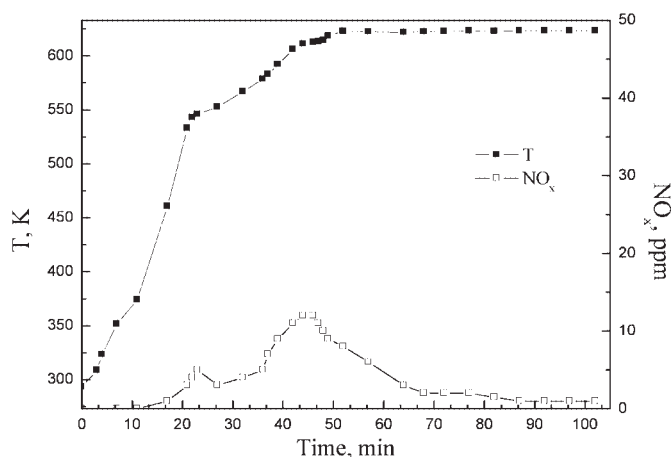
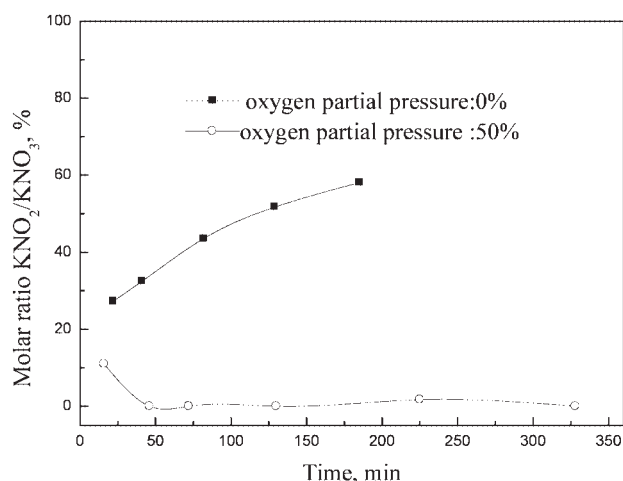


Figure 14. Molar ratio of  $\text{KNO}_2$  to  $\text{KNO}_3$  of original value versus reaction time.

$$1 - 3(1 - f)^{2/3} + 2(1 - f) = 2.081 \times 10^2 \times e^{-\frac{55630}{RT}t} \quad (19)$$

### Behavior of potassium nitrate

As mentioned in previous part, with the addition of potassium nitrate, the system of  $\text{KOH-KNO}_3\text{-H}_2\text{O}$  is made which has lower melting point than  $\text{KOH-H}_2\text{O}$  system.  $\text{KNO}_3$  plays important role in ensuring high-chromium conversion ratio when lower  $\text{KOH}$  amount is used. To enclose the mechanisms of chromite ore decomposition in the system, the reaction behavior of potassium nitrate was investigated.

Under the conditions of temperature  $350^\circ\text{C}$ , stirring speed 700 rpm,  $\text{KOH}$ -to-chromite ore ratio 2:1,  $\text{KNO}_3$ -to-chromite ore ratio 0.8:1, such issue as  $\text{KNO}_2$  (product of potassium nitrate decomposition<sup>16</sup>) content in the system was detected with high purity Ar gas and gas of oxygen partial pressure 50% (gas flow 1 L/min). As shown in Figure 14,  $\text{KNO}_2$  content in the system keeps increasing with reaction time when high purity Ar gas is applied as a protecting atmosphere. However,  $\text{KNO}_2$  appears only in the first reaction period with lower content and keeps nearly zero under the atmosphere with oxygen partial pressure of 50%. This indicates

that  $\text{KNO}_3$  is decomposing during the reaction between chromite ore and the system and oxygen is dissolving into  $\text{KOH-KNO}_3\text{-H}_2\text{O}$  melt first before making an equilibrium. In addition,  $\text{NO}_x$  content of the venting gas was examined with a nitrogen-oxygen analyzer (Figure 14). The  $\text{NO}_x$  content in venting gas is  $<15$  ppm and becomes nearly zero in the later reaction stage.

Combining the results in Figure 14 and previous analysis, the reaction behavior of potassium nitrate can be concluded as Reactions 20 and 21 and shown in Figure 15. At the first period, potassium nitrate reacts with chromite ore and  $\text{KNO}_2$  is generated. In the presence of oxygen, Reaction 21 carries out and  $\text{KNO}_2$  is oxidized into potassium nitrate.

During the process,  $\text{KNO}_3$  can be considered as an inorganic catalyst to enhance the decomposition of chromite ore. However, the role and detailed mechanisms of potassium nitrate need to be further investigated.

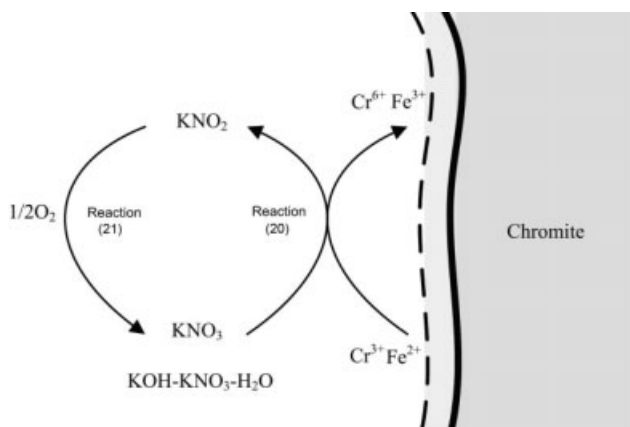
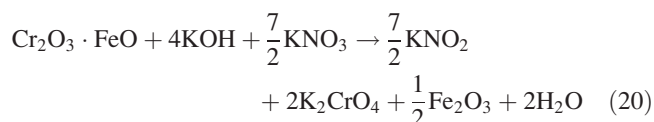


Figure 15. Reaction mechanisms of potassium nitrate in  $\text{KOH-KNO}_3\text{-H}_2\text{O}$  system.

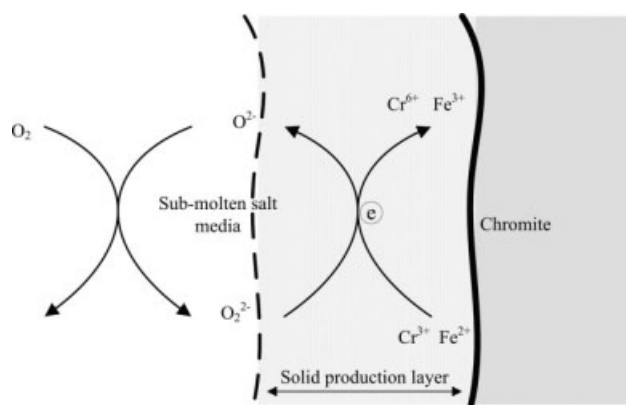
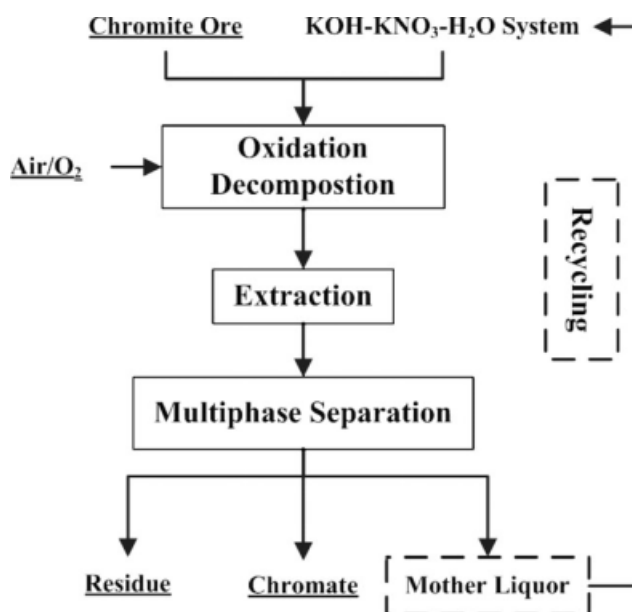


Figure 16. Plot of reactions between  $\text{O}_2^-$  and the surface of chromite.



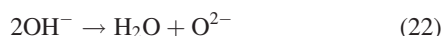


**Figure 17. Principle flow sheet of chromate production with KOH-KNO<sub>3</sub> binary submolten salts.**

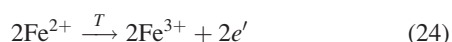
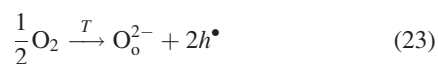
#### *Micromechanisms of chromite ore decomposing in KOH-KNO<sub>3</sub>-H<sub>2</sub>O system*

Chromite ore is a spinel structure with O<sup>2-</sup> frame of cubic-closed-packed (CCP) where Fe<sup>2+</sup> occupies tetrahedral positions and Cr<sup>3+</sup> octahedral positions. In the system of KOH-KNO<sub>3</sub>-H<sub>2</sub>O, the surface of chromite ore is first destroyed and reactants from the melt diffuse into the reacting interface. In addition, at temperatures of around 300°C, the diffusion of Cr<sup>3+</sup> and Fe<sup>2+</sup> from spinel lattice is very weak and can be neglected.<sup>26</sup>

In KOH solution of high concentration or KOH melt, an acid-base equilibrium exists and is shown in Eq. 22.<sup>30</sup>

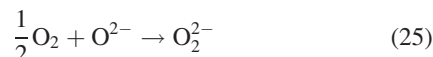


During decomposition of chromite ore in soda ash roasting process, oxygen and Fe<sup>2+</sup> on the surface reacts and new O<sup>2-</sup> sublattice generates along the vacancies of cations (Reactions 23–24). This indicates the oxidation of chromite ore has inevitably relationship with O<sup>2-</sup>. Besides, Fe<sup>2+</sup> on chromite ore surface can contact with oxygen directly in roasting process. However, in KOH-KNO<sub>3</sub>-H<sub>2</sub>O system where liquid is the main phase, the decomposition of chromite ore is a typical solid-liquid-gas three-phase process and the dissolution of oxygen needs existing via O<sup>2-</sup>.



where O<sub>o</sub><sup>2-</sup> is oxygen anion in chromite ore lattice.

The dissolution of oxygen into KOH-KNO<sub>3</sub>-H<sub>2</sub>O system via Reaction 5 can be explained as Eq. 25 and forming a estimated cluster O<sub>2</sub><sup>2-</sup>. It may be a reason of the experimental evidence from Ref. 21, which indicates strong decomposition characters of KOH-H<sub>2</sub>O system when combining with oxygen. Reaction 25 also shows an increase of oxygen dissolution can enhance the decomposition rate of chromite ore.



In the process of chromite ore decomposition, O<sup>2-</sup> around chromite ore particle attacks its surface by Reaction 26 which increases aberration and makes it easier for spinel structure destruction. After the dissolution of oxygen, O<sub>2</sub><sup>2-</sup> oxidizes cations along the aberration and a solid product layer forms.



Therefore, the decomposition can be concluded by Figure 16 where KOH-KNO<sub>3</sub>-H<sub>2</sub>O system performs as a transportation media of oxygen as well as a reactant.

#### *Development of a new chromate production process*

Based on previous theoretical and experimental results, a new process for chromate production from chromite ore by using KOH-KNO<sub>3</sub>-H<sub>2</sub>O system can be proposed with an optimization of the process proposed in Ref. 21. The new process is schematically plotted in Figure 17.

After separation, crude potassium chromate and ferro-rich residue are obtained under similar separation conditions in Ref. 20. The mother liquor containing KOH and KNO<sub>3</sub> are recycled into the next matter cycle. The composition and scanning electron microscope image of the crude potassium chromate crystal (reaction conditions are temperature 350°C, stirring speed 700 rpm, KOH-to-chromite ore ratio 2:1, KNO<sub>3</sub>-to-chromite ore ratio 0.8:1, gas flow 1 L/min, and oxygen partial pressure 50%) are shown in Table 4 and Figure 18, respectively. It shows only very few KNO<sub>3</sub> existing in the final product which crystallizes well with size of around 100 μm.

#### **Conclusions**

A new chromate production process is proposed and proved feasible in the work with a new reaction system of KOH-KNO<sub>3</sub>-H<sub>2</sub>O.

- Different parameters such as KOH-to-chromite ore ratio, KOH-to-chromite ore ratio, temperature, oxygen partial pressure, stirring speed, and gas flow influence the decomposition and chromium conversion ratio of chromite ore. Among them, KOH-to-chromite ore ratio, temperature and oxygen partial pressure are the most important determining reaction rate in the first decomposition period and influencing mass

**Table 4. Composition of the Crude Potassium Chromate Crystal**

Contents	K <sub>2</sub> CrO <sub>4</sub>	Fe <sub>2</sub> O <sub>3</sub>	MgO	MnO <sub>2</sub>	Al <sub>2</sub> O <sub>3</sub>	SiO <sub>2</sub>	CaO	TiO <sub>2</sub>	KOH	KNO <sub>3</sub>
wt %	94.31	0.49	0.12	0.18	0.27	0.27	0.19	0.049	3.01	0.13

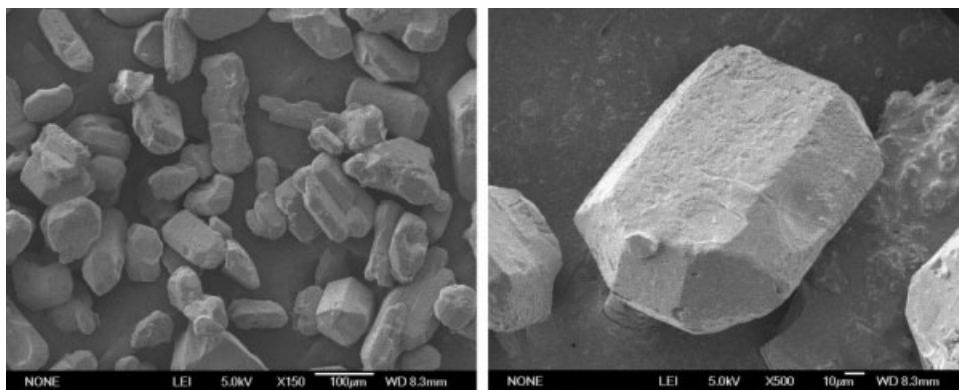


Figure 18. SEM patterns of crude potassium chromate crystal.

transportation in the later period. Under conditions of temperature 350°C, KOH-to-chromite ore ratio 2:1, stirring speed 700 rpm, KNO<sub>3</sub>-to-chromite ore ratio 0.8:1, oxygen partial pressure 50%, and gas flow 1 L/min, >98% of chromium conversion ratio can be obtained with reaction time around 300 min.

- The decomposition of chromite ore particles in KOH-KNO<sub>3</sub>-H<sub>2</sub>O system is a typical process of solid-liquid reaction with a decreasing of reaction surface area and thickening of product layer of solid. Two obvious stages can be observed from the experimental results: a faster reacting stage and a diffusion dominating stage. In the later stage, the solid product layer inhibits the diffusion of KOH and oxygen and a flat stage appears. From macrokinetics investigation, a shrinking unreacted core model can be used to describe the decomposition process, which is coordinately controlled by mass diffusion in the product layer and interface reaction. Apparent activation energy of chromite ore decomposition in the temperature range from 280 to 370°C is 55.63 kJ/mol.

- Potassium nitrate plays a role of catalyst in the oxidation decomposition reaction of chromite ore and potassium hydroxide. The content of KNO<sub>2</sub> increases with the increase of reaction time under inert atmosphere. However, only in the first period of reaction is KNO<sub>2</sub> detected when 50% oxygen partial pressure is applied.

- During reaction, oxygen needs to dissolve into the KOH-KNO<sub>3</sub>-H<sub>2</sub>O melt system first and some cluster with oxidizing characters, e.g. O<sub>2</sub><sup>2-</sup>, is formed. The binary submolten salt system can be considered as a media of oxygen transportation and reactant donator.

## Acknowledgments

Zhi Sun thanks Ms. Guo Xiaoling for the brilliant and useful suggestions. This work was supported by the National Science and Technology Pillar Program of China (Grant No. 2006BAC02A05), the National Science Foundation of China (Grant No. 50234040), and the National Basic Research Program (973 Program) of China (Grant No. 2007CB613501).

## Literature Cited

- Kanagaraj J, Chandra Babu NK, Mandal AB. Recovery and reuse of chromium from chrome tanning waste water aiming towards zero discharge of pollution. *J Clean Prod.* 2008;16:1807–1813.
- Abdeen MO. Energy, environment and sustainable development. *Renew Sustain Energy Rev.* 2007;12:2265–2300.
- Trost BM. Atom economy: a search for synthetic efficiency. *Science.* 1991;254:1471–1477.
- Zhang Y. The green process engineering science. *Chinese J Process Eng.* 2001;1:10–15.
- Ding Y, Ji Z. *Production and Applications of Chromium Compounds.* Beijing: Chemical Industry Press, 2003.
- NRC Committee. Chromium, medical and biological effects of environmental pollutants. *Report of Committee on Biological Effects of Atmospheric Pollutants, Division of Medical Sciences.* Washington, DC: National Research Council, 1974.
- Shi PY. *The Study on Cleaning Process of Preparation of Alkaline Chromium Sulfate by Sulfuric Acid Leaching of Chromite.* Master Thesis. University of Northern-East, Shenyang, P.R. China, 2002.
- Geveci A, Topkaya Y, Ayhan E. Sulfuric acid leaching of Turkish chromite concentrate. *Miner Eng.* 2002;15:885–888.
- Clay JL, Pearce JF, Trethewey DH. An acid process for the production of chromic anhydride from chromite ore. *J Soc Chem Ind.* 1950; 69:275–282.
- Udy MJ. *Chromium: Chemistry of Chromium and Its Compounds, Vol. 1.* New York: Reinhold Publishing Corporation, 1956.
- Kowalski Z, Mazanek C. Sodium chromate-material flow analysis and technology assessment. *J Clean Prod.* 1998;6:135–142.
- Charles PB, William WL, Edmund WS. Process for the production of sodium chromate from chromite ore. U.S. Pat. 3,852,059, 1974.
- Arnadta U, Batza M, Bellinghausena R, Blocka HD, Helkera H, Lonhoffa N, Moretto HH, Nieder-Vahrenholza HG, Rinkesa H, Spreckelmeyera B, Webera R. Method for manufacturing alkaline chromates from chromite ore. *Miner Eng.* 1996;9:1183.
- Chandra D, Wang GX, Fuerstenau MC, Siemens RE. Alkali roasting of low-grade chromite. *Trans Instn Min Metall (Section C: Mineral Process Extr Metall.)*. 1996;105:C105–C112.
- Hundley GL, Nilsen DN, Siemens RE. Extraction of Chromium from domestic chromite by alkali fusion. *U.S. Bureau of Mines, Report of Investigations, RI8977.* U.S. Bureau of Mines, Pittsburg, U.S., 1985.
- Kashiwase K, Sato G, Atumi T, Okabe T. Appropriate oxidizing conditions of chromite with molten sodium salts. *Nippon Kagaku Kaishi.* 1974;3:469–473.
- Kanari N, Gaballah I, Allain E. A study of chromite carbochlorination kinetics. *Metall Mater Trans B.* 1999;30:577–587.
- Kanari N, Gaballah I, Allain E. Kinetics of oxychlorination of chromite. I. Effect of temperature. *Thermochim Acta.* 2001;371:143–154.
- Kanari N, Gaballah I, Allain E. Kinetics of oxychlorination of chromite. II. Effect of reactive gases. *Thermochim Acta.* 2001;371:75–86.
- Xu HB, Zheng SL, Zhang Y, Li ZH, Wang ZK. Oxidative leaching of a Vietnamese chromite ore in highly concentrated potassium hydroxide aqueous solution at 300°C and atmospheric pressure. *Miner Eng.* 2005;18:527–535.
- Zhang Y, Li ZH, Qi T, Zheng SL, Li HQ, Xu HB. Green manufacturing process of chromium compounds. *Environ Prog.* 2005;24:44–50.
- Zheng SL, Zhang Y, Li ZH, Qi T, Li HQ, Xu HB. Green metallurgical processing chromite. *Hydrometallurgy.* 2006;82:157–163.

23. Sun Z, Zheng SL, Zhang Y. Thermodynamics study of the decomposition of chromite with KOH. *Acta Metall Sinica (Engl Lett)*. 2007;20:187–192.
24. Sun Z, Zheng SL, Xu HB, Zhang Y. Oxidation decomposition of chromite ore in molten potassium hydroxide. *Int J Miner Process*. 2007;83:60–67.
25. Du CH. Fundamental and Application Research of Phase Equilibrium of Sub-molten Salt Media in Clean Process of Chromite Ore. Ph.D. Thesis. Institute of Process Engineering, Chinese Academy of Sciences, Beijing, China, 2007.
26. Tathavadkar VD, Antony MP, Jha A. The physical chemistry of thermal decomposition of South African chromite minerals. *Metall Mater Trans B*. 2005;36:75–84.
27. Mo DC. *Kinetics of Metallurgy*. Changsha: South China University Press, 1985.
28. Li WC. *Physical Chemistry of Metallurgy and Materials*. Beijing: Metallurgical Engineering Press, 2006.
29. Brandes EA. *Smithells Metals Reference Book*. London: Butterworths, 1983.
30. Duan SZ, Qiao ZY. *Molten Salt Chemistry*. Beijing: Metallurgical Engineering Press, 1990.

*Manuscript received Sep. 15, 2008, revision received Dec. 8, 2008, and final revision received Jan. 31, 2009.*